PAGEOPH, Vol. 142, No. 2 (1994) 0033-4553/94/020329-18$1.50 + 0.20/0

Effect of Basal Guided Waves on Landslides

YOSHIMASA KOBAYASHI[1]

Abstract—A landslide model riding on basal guided waves is investigated to explain lower net frictions at high slide velocities from the wave-theoretical point of view. It is shown that there is a wave propagated along the basal layer at the phase velocity equal to the slide velocity, as well as a guided wave with considerably higher phase velocities propagated likewise along the basal layer as a leaking mode at low slide velocities. With increasing slide velocity the phase velocity of the guided wave decreases until it is equal to that of the slide mass. Over this threshold slide velocity, a "sonic boom" is generated around the basal layer, and the shock contributes to a loosening of the slide mass into a fluidized state. Landslides on long slide-ways are more liable to exceed this threshold velocity since their slide velocities tend to be higher than those on short slide-ways of a similar shape. Hence, the reduction of net friction of landslides can possibly be better correlated with the lengths of slide-ways than with the volumes of landslides as is widely maintained.

Key words: Landslide, wave theory, guided wave, threshold slide velocity, sonic boom, mechanical fluidization.

Introduction

SCHEIDEGGER (1973) pointed out an observation that the net friction (the tangent of a slope connecting the top of the slide scarp and the toe of the stopped slide mass) is lower in larger landslides than in smaller ones (Fig. 1). This phenomenon suggests that there is some mechanism that reduces slide resistance more strongly in larger landslides than in smaller ones. Many hypotheses have been proposed to explain the mechanism for this reduced net friction in large-scale landslides. The hypotheses are either those which assume some lubrication media such as air (KENT, 1966; SHREVE, 1968), pore-water (ASHIDA and EGASHIRA, 1986; SASSA, 1988), etc. (HABIB, 1975), or those which assume effects of some dynamic phenomena such as acoustic fluidization (MELOSH, 1979), or basal pressure waves (FODA, 1993).

In view of long runout landslides observed in various conditions which span dry to wet environments, including those on the earth as well as on planets where no

[1] Aso Volcanological Laboratory, Faculty of Science, Kyoto University, Choyo, Aso, Kumamoto 869-14, Japan.

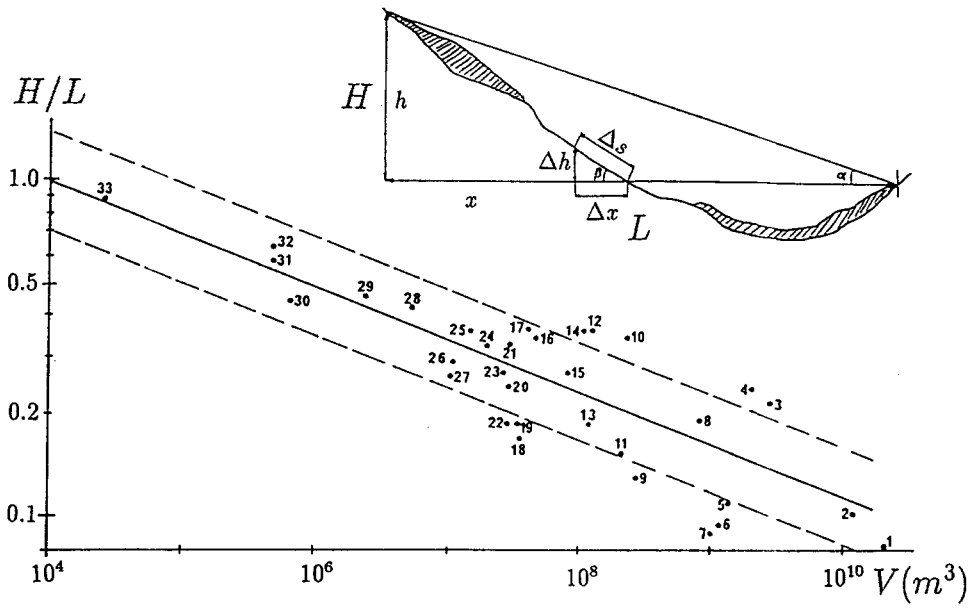

Figure 1
Correlation between the volume of landslide and the net friction angle (height dropped/horizontal distance travelled). (Modified from SCHEIDEGGER, 1973.)

sufficient quantity of lubricant such as air or water can be expected (MELOSH, 1986), it is possible to assume a mechanism that needs no lubricating materials to reduce slide resistance. The hypothesis of acoustic fluidization by MELOSH (1979) is one of such mechanisms and that of basal pressure waves by FODA (1993) is another. The former is interesting, since it assumes a mechanism that facilitates a flow of granular material through temporal as well as spatial stress relieving by acoustic waves in the sliding mass, however it has not explained how the acoustic energy is generated in landslide masses: The latter has a desirable feature since it concentrates on the mechanism for generating basal waves which are related to the decrease of energy dissipation during sliding. FODA (1993) has shown the existence range of such waves theoretically, but the characteristics of the waves are not yet fully understood, and hence this hypothesis deserves further examination.

In the present study, therefore, I will examine Foda's hypothesis from a wave-theoretical point of view and examine in detail the characteristics of the waves predicted by the model. After the examination I will discuss briefly the effect of the basal waves on the behavior of landslides of various sizes.

Formulation and Solution of the Basal Waves

FODA (1993) examined whether a *Kelvin-Helmholtz* type instability can occur on the boundary between a thin basal layer underlain by the rigid basement and the

overlying elastic solid half-space corresponding to landslide mass (Fig. 2). He demonstrated theoretically that unstable waves can arise at the boundary when the slide velocity of the overlying mass exceeds a threshold value.

According to FODA (1993), we employ the two-dimensional *Euler* system (fixed to the space) and taking the x axis in the direction of sliding the equations of motion of the elastic solid are

$$\rho\left(\frac{\partial^2 u}{\partial t^2}+U\frac{\partial^2 u}{\partial t\,\partial x}\right)=G\left(\nabla^2 u+\frac{1}{1-2v}\frac{\partial\dot{\Theta}}{\partial x}\right)$$
$$\rho\left(\frac{\partial^2 w}{\partial t^2}+U\frac{\partial^2 w}{\partial t\,\partial x}\right)=G\left(\nabla^2 w+\frac{1}{1-2v}\frac{\partial\dot{\Theta}}{\partial z}\right), \tag{1}$$

where u and w are particle velocities in x and z directions, the z axis being taken perpendicular to the x axis upward, ρ the density, G the rigidity, v the Poisson's ratio, $\dot{\Theta}$ the dilatation rate, and U the slide velocity of the landslide mass, respectively (see Fig. 2). The relations between stress rates and strain rates are

$$\dot{\sigma}_x=G\left(2\frac{\partial u}{\partial x}+\frac{2v}{1-2v}\dot{\Theta}\right)$$
$$\dot{\tau}_{xz}=G\left(\frac{\partial u}{\partial z}+\frac{\partial w}{\partial x}\right) \tag{2}$$
$$\dot{\sigma}_z=G\left(2\frac{\partial w}{\partial z}+\frac{2v}{1-2v}\dot{\Theta}\right).$$

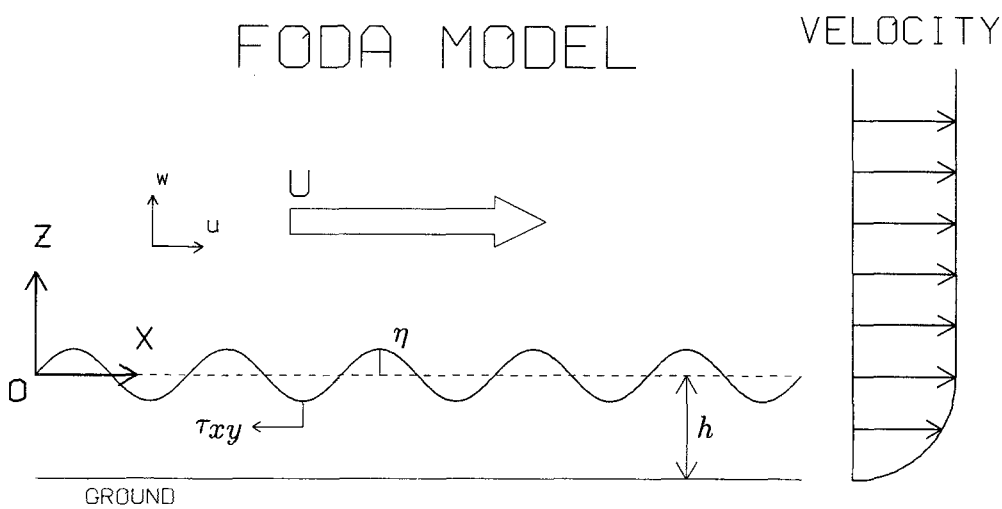

Figure 2
A model after FODA (1993). A horizontally sliding elastic half-space is underlain by a thin boundary layer sitting on the rigid basement. The boundary layer behaves as a granular material. An instability is expected to occur between the elastic body and the boundary layer.

In the basal layer it is assumed that the medium behaves as a mass of granular material, and that the following relations hold for horizontal velocity fluctuation u_0 and vertical pressure in the basal layer p_z (both in a very thin basal layer do not depend on z), as well as the vertical displacement η on the boundary between the elastic solid and the basal layer,

$$\begin{aligned} \rho\, \partial u_0/\partial t &= -\bar{\kappa}\, \partial p_z/\partial x \\ \partial \eta/\partial t + h\, \partial u_0/\partial x &= 0, \end{aligned} \tag{3}$$

where $\bar{\kappa}$ is the reduced coefficient of lateral earth pressure, $\bar{\kappa} = \kappa - K^2$, κ and K being the coefficients of lateral earth pressure and of friction in the basal layer respectively, and h the thickness of the basal layer (FODA, 1993) (Appendix 1).

If no disturbance is given on the boundary between the basal layer and the overlying slide mass, the above relations are solved under the following boundary conditions at $z = 0$:

$$\begin{aligned} w &= \partial \eta/\partial t + U\, \partial \eta/\partial x \\ \sigma_z &= -p_z \\ \tau_{xz} &= K p_z, \end{aligned} \tag{4}$$

and for infinitely large z

$$u, w \to 0.$$

We introduce two-dimensional velocity potentials ϕ and ψ as follows:

$$\begin{aligned} u &= \partial \phi/\partial x - \partial \psi/\partial z \\ w &= \partial \phi/\partial z + \partial \psi/\partial x. \end{aligned} \tag{5}$$

If we assume ϕ and ψ in the forms

$$\begin{aligned} \phi &= A \exp(-az + ikx - i\omega t) \\ \psi &= B \exp(-bz + ikx - i\omega t), \end{aligned} \tag{6}$$

and substitute them into (5) and (1), a and b should satisfy

$$\begin{aligned} a^2 &= k^2 - (\omega^2 - k\omega U)/c_p^2 \\ b^2 &= k^2 - (\omega^2 - k\omega U)/c_s^2, \end{aligned} \tag{7}$$

where $c_p^2 = (\lambda + 2\mu)/\rho$ and $c_s^2 = \mu/\rho$.

To be consistent with ϕ and ψ, all variables are assumed to be proportional to $\exp(ikx - i\omega t)$, i.e.,

$$\begin{aligned} \eta &= C \exp(ikx - i\omega t) \\ p_z &= p_0 \exp(ikx - i\omega t). \end{aligned} \tag{8}$$

By using (3) we obtain

$$C = (kh\bar{\kappa})kp_0/(\rho\omega^2). \tag{9}$$

The physical meaning of the assumed functions in (6) and (8) is a wave propagating along the boundary between the elastic half-space and the basal layer at a wave number k and a frequency ω.

Substituting u, ω, η and p_z into the boundary conditions (4), we have the simultaneous equations in terms of p_0, A and B,

$$\begin{aligned} (-i\omega + ikU)(kh\bar{\kappa})kp_0/(\rho\omega^2) + aA - ikB = 0 \\ i\omega p_0 + 2G(vk^2 + (1-v)a^2)A/(1-2v) + 2iGkbB = 0 \\ -i\omega Kp_0 + 2iakGA + (k^2+b^2)GB = 0. \end{aligned} \tag{10}$$

If a disturbance is given on the boundary, the right-hand side of (10) is a nonzero vector corresponding to the disturbance given, and the solutions for p_z, ϕ or ψ have the form such as

$$p_z, \phi \text{ or } \psi = \int_{-\infty}^{\infty} \int_{-\infty}^{\infty} \frac{G(k,\omega)}{F(k,\omega)} \exp i(kx - \omega t)\, dk\, d\omega \tag{11}$$

where $F(k, \omega)$ is the determinant made of the coefficients of (10):

$$F(k,\omega) = \begin{vmatrix} (-i\omega + ikU)(kh\bar{\kappa})k/(\rho\omega^2) & a & -ik \\ i\omega & 2G(vk^2-(1-v)a^2)/(1-2v) & 2iGkb \\ -i\omega K & 2iakG & (k^2+b^2)G \end{vmatrix}, \tag{12}$$

and $G(k, \omega)$ is the determinant made from $F(k, \omega)$ by replacing the first, second or third column for p_z, ϕ or ψ respectively by the vector in the right-hand side of (10).

So as to examine the solution for (11), we consider the integration in terms of ω while k is kept fixed, e.g.,

$$\bar{\phi}(k, t) = \int_{-\infty}^{\infty} \frac{G(k,\omega)}{F(k,\omega)} \exp(-az + ikx - i\omega t)\, d\omega, \tag{13}$$

where $\bar{\phi}(k, t)$ is the Fourier transform of $\phi(x, t)$ in terms of space x.

Major contributions of an integral of the form (13) will be given by the poles of the integrand, and we examine the zeros of the denominator,

$$F(k, \omega) = 0. \tag{14}$$

In the case of $\nu = 0.25$ this yields the characteristic equation in a nondimensional form,

$$F(k, \omega)/\omega b^3 = -i(1 - kU/\omega)(kh\bar{\kappa})(c_s b/\omega)^2(k/b) * [\{(k/b)^2 - 3(a/b)^2\}\{(k/b)^2 + 1\} + 4(k/b)^2(a/b)] + i[(k/b)^2 - 1](a/b) + K[(k/b)^2 - 3(a/b)^2](k/b) + 2K(k/b)(a/b) = 0. \quad (15)$$

The problem to be examined pertains to the kind of roots the characteristic equation may have, and if it has real roots of ω for a fixed k, it implies that the assumed wave can exist as a sustaining (normal) mode. Considering that the time dependence of the assumed functions is $\exp(-i\omega t)$, the contour integral should be conducted in the lower half plane, and hence the complex roots of (15) in the negative-imaginary ω area will contribute the integral as decaying waves (Appendix 2).

Waves Predicted by the Basal-wave Model

In the previous section we have derived the characteristic equation for the basal wave proposed by Foda. Here, we will examine the waves predicted by the model.

First, we will simply touch upon the body waves with the wave number k that can be excited in the elastic half-space. In integral representation of waves (13), body waves are evaluated by branch line integrals encircling the branch points given by the zeros of (7). They will yield the phase velocities of $c = \omega/k \simeq U/2 \pm c_p$ and $c = \omega/k \simeq U/2 \pm c_s$ for $U \ll c_s$, which show a kind of *Doppler* effect, depending on the direction of propagation. They are P and S waves (homogeneous waves) along the boundary in the elastic body.

Next, we examine the absolute value of the characteristic equation (the denominator of the integrand) $|F|$. When the denominator of a function has a minimum at a point while the numerator remains stable, the function will pose a peak that must be either a smooth mound, saddle point or pole. On the other hand, an analytic complex function can never have smooth mounds, and therefore if there is no such indication of a saddle point, the minimum of the denominator must give a pole.

We can see that $|F|$ has a minimum (zero) in the negative-imaginary ω area for slide velocity $U = 0$ (Fig. 3). In calculating the characteristic equation, parameters

Figure 3

Diagrams showing the zero of the characteristic equation $F = 0$ for the guided wave along the basal layer when the slide velocity is zero for the cases of the basal layer thicknesses; a) $h = 0.1$ m, b) $h = 0.2$ m and c) $h = 0.5$ m. S-wave velocity is 150 m/s and Poisson's ratio is 0.25. The wave number k is fixed at 1.0 m^{-1}. Contour lines are for $|F|$ in arbitrary scale. Minima are indicated by L.

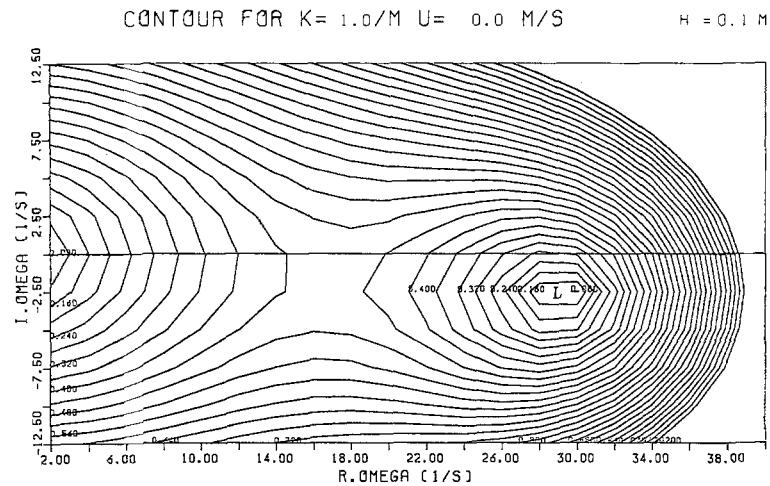
CONTOUR FOR K= 1.0/M U= 0.0 M/S
H =0.1 M
I.OMEGA (1/S)
R.OMEGA (1/S)
12.50
7.50
2.50
-2.50
-7.50
-12.50
2.00
6.00
10.00
14.00
18.00
22.00
26.00
30.00
34.00
38.00

a)

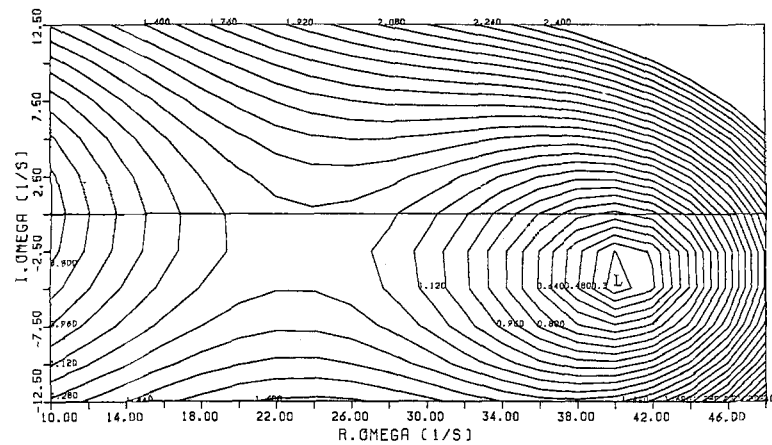
CONTOUR FOR K= 1.0/M U= 0.0 M/S
H =0.2 M
I.OMEGA (1/S)
R.OMEGA (1/S)
12.50
7.50
2.50
-2.50
-7.50
-12.50
10.00
14.00
18.00
22.00
26.00
30.00
34.00
38.00
42.00
46.00

b)

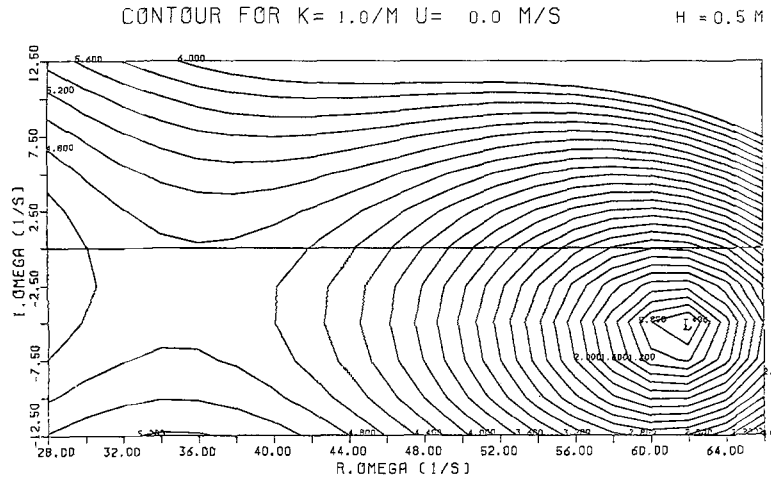
CONTOUR FOR K= 1.0/M U= 0.0 M/S
H =0.5 M
I.OMEGA (1/S)
R.OMEGA (1/S)
12.50
7.50
2.50
-2.50
-7.50
-12.50
28.00
32.00
36.00
40.00
44.00
48.00
52.00
56.00
60.00
64.00

c)

for the elastic body and the basal layer are assumed as follows: S-wave velocity = 150 m/s and $\nu = 0.25$, and for the basal layer $k = 1.0\ \mathrm{m}^{-1}$ (wavelength of $2\pi/k = 6.28$ m) and $h = 0.1$, 0.2 and 0.5 m. The reduced coefficient of lateral earth pressure $\bar{\kappa}$ and the coefficient of friction K are assumed to be 0.3 and 0.6 (corresponding to $\kappa = 0.66$), respectively. The parameters in the following calculations are always the same if not stated otherwise. The minimum in the contour map corresponds to a guided wave in the basal layer. It resembles a leaking mode, because the pole of (13) with a small imaginary part of ω represents a normal-mode wave plus body waves that are propagated away from the basal layer into the upper elastic half-space (see Appendix 2). It may be interpreted that the energy of the guided wave leaks in the elastic half-space and it would decay if additional energy was not supplied during sliding successively. The values for the real part of ω are about 29, 40 to 55 s^{-1} for $k = 1.0\ \mathrm{m}^{-1}$, i.e., the phase velocities are about 29, 40 to 55 m/s depending on the thicknesses $h = 0.1$, 0.2 and 0.5 m, respectively. This dependency of the velocity on the thickness is analogous to that of long waves in shallow water whose velocities are higher in deeper water.

Now, let's turn to the cases for nonzero slide velocities. So far, in the analysis using the function $\exp(ikx - i\omega t)$, we have intuitively assumed that k and ω as well as U are positive. We will examine here the waves propagated in and against the direction of sliding. A comparison of the cases for two equal U's, but with the opposite sign, is shown in Figure 4. The thickness of the basal layer is 0.1 m. It is interesting to note that both contour maps give similar poles in the negative ω area but slightly different angular frequencies. This difference is caused partly by the *Doppler effect* on propagation of the guided waves toward $\pm U$, respectively and partly by an effect of the slide velocity U on the characteristic equation F of (15).

The above discussion demonstrates that the waves predicted by the *Foda* model are physically reasonable, and we will see the effect of slide velocity on the basal waves in the next section.

Effects of Slide Velocity on the Basal Waves

The loci of the poles for various slide velocities are shown in Figure 5. In the low U range (U up to about 10 m/s), it is noted that there are in general two poles: one on the real ω axis and the other in the negative-imaginary ω area. The imaginary part of the latter is not large and the dissipation is presumed to be small. As the slide velocity is increased, the former pole is shifted to the right on the real ω axis to the angular frequency corresponding to the phase velocity equal to the slide velocity U, i.e., $c = \omega/k = U$. It is easy to see from (15) and (7) that as far as ω remains real, $\omega = kU$ always gives a root of $F = 0$. This corresponds to the wave that is propagated at the velocity equal to that of the landslide mass. The latter pole is shifted to the left, i.e., to a lower frequency with increasing slide velocity.

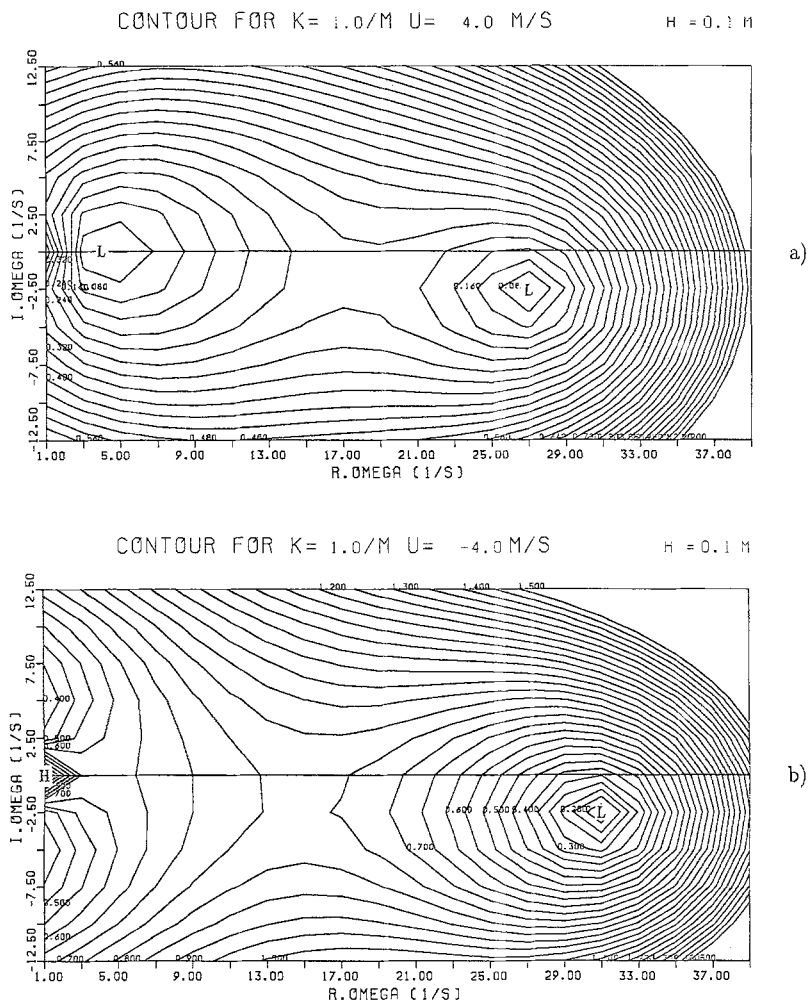

Figure 4

Diagrams showing the zeros of the characteristic equation $F = 0$ for positive and negative slide velocities, $U = \pm 4.0$ m/s. The wave number k is 1.0 m^{-1} and the layer thickness is 0.1 m. Other parameters are the same as in Fig. 3. Contour lines are for $|F|$ in arbitrary scale. Minima are indicated by L and maxima by H.

Thus, both poles approach each other first with the increase in the slide velocity, but at a certain slide velocity, at about 11 to 12 m/s in the present case, the second (complex) pole begins to deflect downward, while the first (real) pole continues to move to the right on the real ω axis. The guided waves after this downward deflection are more dissipative than in lower slide velocities. At this velocity the third pole appears in the positive-imaginary ω area: this does not contribute to the integral as is shown in Appendix 2. It is difficult to determine exactly at which

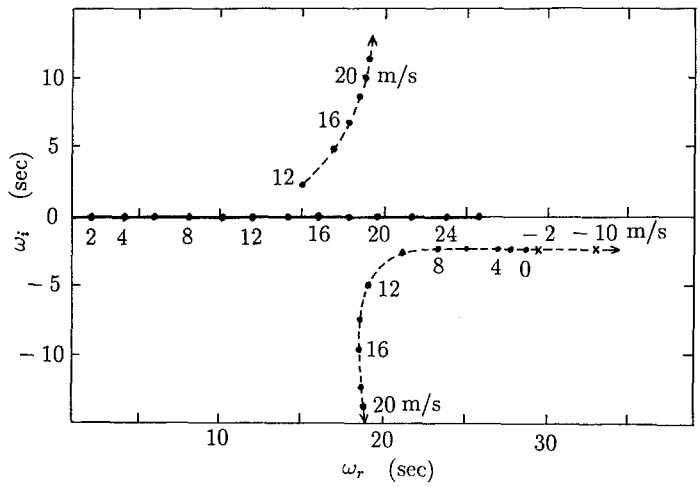

Figure 5

Loci of zeros of the characteristic equation $F = 0$ for various slide velocities, U. Numbers attached to dots on the loci are the velocity of the slide that gave the zeros. There are three loci connecting the zeros with a negative-imaginary part of ω and those on the real ω axis for low slide velocities as well as those with a positive-imaginary part of ω that appear only for high slide velocities. Parameters except the slide velocity are the same as in Figure 3.

frequency the phenomenon described above occurs, however around this sliding velocity, the guided wave with a negative-imaginary ω part is caught up with the wave at the velocity U which is being propagated with the sliding mass.

In the elastic wave theory it is known that the stresses caused by a moving surface load increase drastically as the velocity of the load approaches that of the Rayleigh wave (EASON, 1965). If this principle can be applied to the present model even though the guided waves in high slide velocities are rather dissipative compared to Rayleigh waves, a "sonic boom" is expected to be generated in the basal zone of the slide; this occurs because over this slide velocity the effect of the disturbance given to the base of a landslide at a location fixed to the reference cannot be propagated away in the forward direction in the form of the guided wave any more and the energy must be accumulated near the wave front with lapse of time.

Thus, there is a threshold velocity to generate a "sonic boom" corresponding to an assumed wave number k. For higher positive slide velocities, a shock front will be propagated in the forward direction (which is beyond the scope of the present analysis), while in the opposite direction there is still a normal guided wave correponding to the pole located in the negative-imaginary ω area; see Figure 6 for $U = \pm 16$ m/s.

The fact that the pole located on the real ω axis is found only in the map for positive U is natural, since it corresponds to the wave proceeding in pace with the landslide mass.

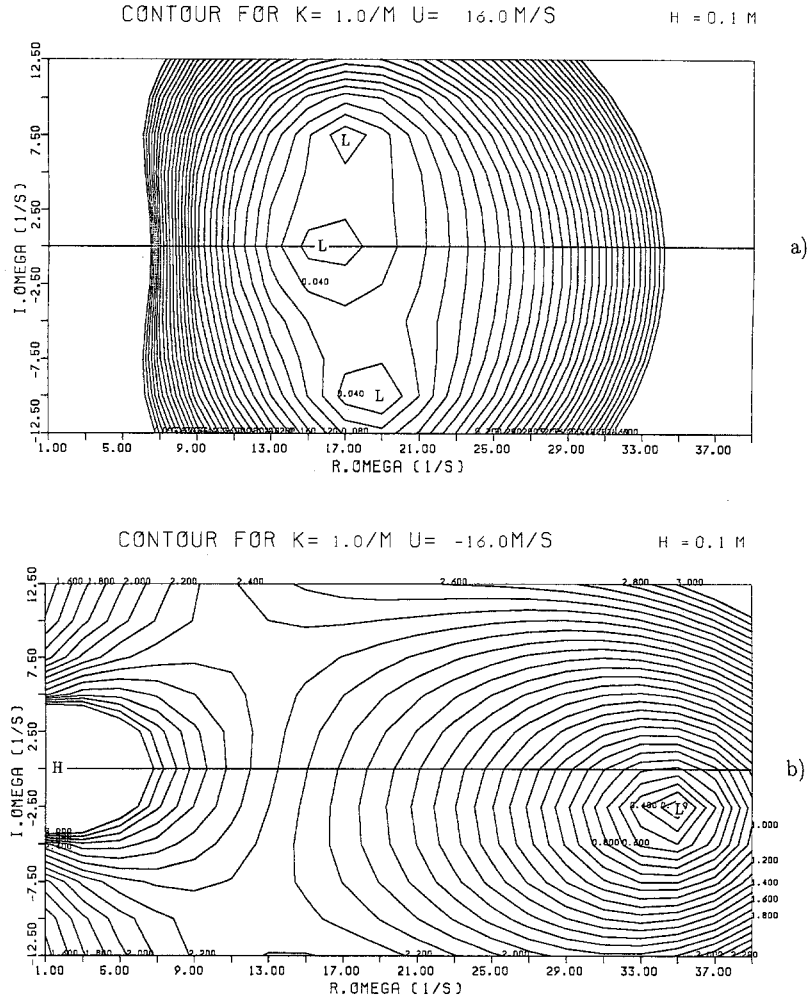

Figure 6

Diagrams showing the zeros of the characteristic equation $F = 0$ for positive and negative slide velocities, $U = \pm 16$ m/s, exceeding the threshold value. The zero on the real ω axis for positive U corresponds to the wave propagated at the velocity equal to that of the landslide mass. This pole is not found for negative U. Parameters are the same as in Figure 4. Contour lines are for $|F|$ in arbitrary scale. Minima are indicated by L and maxima by H.

Discussion on Effects of Basal Waves on Landslides

The analysis in the last section shows a variable effect of the guided wave in the basal part of landslides depending on the slide velocity. It was found that a shock similar to "sonic boom" can arise in the basal zone if the slide velocity exceeds a threshold. This may possibly be responsible for reducing the resistance in landslides.

Although FODA (1993) made an energy calculation accompanying the basal pressure waves to show a smaller energy dissipation being realized at high slide velocities, we will not do this since quantitative evaluation of energy in the supersonic state is in general difficult. Thus, we will discuss the problem here only qualitatively.

Initially we consider two landslides on two long and short geometrically similar slide-ways that have equal coefficients of friction. Denoting the quantities for the slide on the long slide-way by upper-case characters and those on the short one by lower-case characters, the accelerations they acquire under the effect of gravity will be equal to each other, i.e., $A = a$. Under geometrically similar conditions, the attained distances, after sliding up to the corresponding locations on the two similar slide-ways, will be $L > l$. Accordingly, the times needed by the slides on the long and short slide-ways to travel the above distances are respectively $T = \sqrt{2L/A} \propto \sqrt{L}$ and $t = \sqrt{2l/a} \propto \sqrt{l}$. The velocities that the two slide masses will acquire in the time spans above would be $U = \sqrt{2AL} \propto \sqrt{L}$ and $u = \sqrt{2al} \propto \sqrt{l}$, and therefore $U > u$. Hence, even on geometrically similar slopes, a slide on a longer slide-way will have a higher chance to exceed the threshold velocity, since it can acquire higher velocity than that on a shorter slide-way.

If the above reasoning is correct, only the landslide on longer slide-ways will take a different time-distance process after the threshold has been exceeded (Fig. 7), i.e., landslides on small-scale slopes remain normal, while those on large-scale slopes behave abnormally, since a shock wave is excited which in turn contributes to the loosening of rock masses during sliding. As a result, the coefficient of friction only for landslides on originally long slopes is reduced, and the masses travel considerably longer distances than those proportional to the initial coefficients of friction.

It is normally difficult to give direct evidence for the present postulate because of difficulty in data acquisition in real landslides, however there is useful supporting

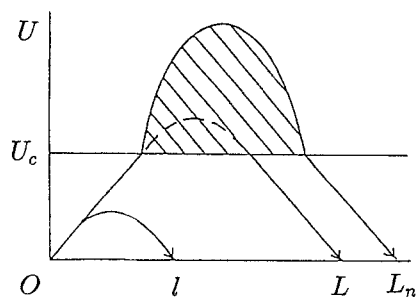

Figure 7

Comparison between slides on long and short geometrically similar slopes. U, L, l are slide speeds, the traveled distances of slides on long and short slide-ways, respectively. Only the slide on long slide-way can exceed a threshold speed U_c, and may travel a larger distance than that anticipated from the usual coefficient of friction.

information: first, this sequence is consistent with DAVIES (1982), who ascribes *Scheidegger*'s finding to the spreading of debris mass caused by "*mechanical fluidization.*" He maintains that high rates of shear in the basal region of a slide are responsible for causing mechanical fluidization with locally high dilation and reduction of internal friction. He maintains this mechanism as a high-velocity extension of BAGNOLD's (1954) results; second, it was observed in the deposits of a debris avalanche that rigid plugs 5 to 7 m thick were underlain by laminar boundary layers 10 to 15 cm thick which seemingly had been under strong shear (TAKARADA, 1991); and third, there are many reports of a great roar or noise having accompanied large debris avalanches or rapid landslides, e.g., Mt. Huascaran in Peru in 1970 (CLUFF, 1971 and PLAFKER *et al.*, 1971), and Mt. Ontake in Japan in 1984 (OKUDA *et al.*, 1985). These noises strongly suggest a self-exciting mechanism for shocks or oscillations in the basal zone of landslides.

Conclusions

The possibility of basal pressure waves proposed by FODA (1993) has been investigated from the wave-theoretical point of view.

Characteristics of the waves predicted by the *Foda* model are investigated and it is found that there are two types of waves excited along the basal layer: the first is a normal-mode wave that is propagated at the velocity equal to that of the landslide; and the second is a decaying wave guided along the basal layer. The latter is caught up with the slide mass in high slide velocities exceeding a threshold. This causes a "sonic boom" phenomenon that may contribute to the loosening of sliding masses.

The slide velocities of landslides on long slopes tend to be higher than those on short slopes of geometrically similar shape, and the velocities on long slopes are more likely to exceed the threshold value which causes the sonic boom than those on short slopes. Long-runout landslides on a gentle slope thus may be explained by the loosening of material caused by a shock wave and reduction of the coefficient of friction of the slide mass as a result of "mechanical fluidization."

Experiences in past landslides such as observed basal layers under plug flows in debris-avalanche deposits as well as a great roar or noise accompanying large debris avalanches support the present postulate.

Appendix 1

We will derive the reduced coefficient of lateral earth pressure $\bar{\kappa}$ only briefly (for details see FODA, 1993). In the basal zone we assume a shear flow U_b in the x direction superposed by perturbation velocities u_1 and u_2 in the x and z directions, respectively, i.e.,

$$\begin{aligned} u &= U_b(z) + u_1 \\ w &= u_2 . \end{aligned} \tag{A1.1}$$

We assume further a basal material to be incompressible,

$$\partial u/\partial x + \partial w/\partial z = 0. \tag{A1.2}$$

The conservation of momentum in the horizontal and vertical directions is expressed by

$$\begin{aligned} \rho(\partial u/\partial t + u\,\partial u/\partial x + w\,\partial u/\partial z) &= -\partial p_x/\partial x + \partial p_{xz}/\partial z \\ \rho(\partial w/\partial t + u\,\partial w/\partial x + w\,\partial w/\partial z) &= \partial p_{xz}/\partial x - \partial p_z/\partial z, \end{aligned} \tag{A1.3}$$

where ρ is the bulk density, and p_x, p_{xz} and p_z are the components of perturbation pressure tensor. If we substitute u and w of (A1.1) in (A1.3), we have as a first approximation

$$\begin{aligned} \rho(\partial u_1/\partial t + U_b\,\partial u_1/\partial x + u_2\,\partial U_b/\partial z) &= -\partial p_x/\partial x + \partial p_{xz}/\partial z \\ \rho(\partial u_2/\partial t + U_b\,\partial u_2/\partial x + u_2\,\partial u_2/\partial z) &= \partial p_{xz}/\partial x - \partial p_z/\partial z. \end{aligned} \tag{A1.4}$$

If we assume a very thin basal zone relative to wavelengths ($2\pi/k$), i.e., $hk \ll 1$, then the left-hand side of the second equation of (A1.4) may be neglected, since $u_2 = O(u_1) * hk$. Thus,

$$\partial p_{xz}/\partial x = \partial p_z/\partial z. \tag{A1.5}$$

Now we try to gain an averaged expression for the basal layer, and to this end we integrate the first expression of (A1.4) in terms fo z. According to FODA (1993) we assume for U_b and u_2 the following relations,

$$\begin{aligned} U_b &= U(z/h) + \sum_{n=1} a_n \sin(2n\pi(z/h)) \\ u_2 &= \partial\eta/\partial t * (z/h) + \sum_{n=1} \sin(2n\pi(z/h)). \end{aligned} \tag{A1.6}$$

Then, it is easy to show

$$\int_0^h (U_b\,\partial u_1/\partial x + u_2\,\partial U_b/\partial z)\,dz = 0. \tag{A1.7}$$

Therefore, the first of (A1.4) is

$$\rho(\partial u_0/\partial t) = -\partial p_x/\partial x + \partial p_{xz}/\partial z, \tag{A1.8}$$

where u_0 is the average of u_1 over the height h.

The right-hand side of (A1.8), $-\partial p_x/\partial x + \partial p_{xz}/\partial z$, can be rewritten by using the relations in the granular material in the basal layer, $p_x = \kappa p_z$ and $p_{xz} = K p_z$, (or $\partial p_x/\partial x = \kappa\,\partial p_z/\partial x$ and $\partial p_{xz}/\partial z = K\,\partial p_z/\partial z$ as well as $\partial p_{xz}/\partial x = K\,\partial p_z/\partial x$) and (A1.5). Thus, the first term of the right-hand side of (A1.8),

$$-\partial p_x/\partial x = -\kappa\,\partial p_z/\partial x$$

and the second term of the right-hand side of (A1.8),

$$\partial p_{xz}/\partial z = K\,\partial p_z/\partial z = K\,\partial p_{xz}/\partial x = K^2\,\partial p_z/\partial x,$$

and finally,

$$\rho(\partial u_0/\partial t) = -(\kappa - K^2)\,\partial p_z/\partial x. \tag{A1.9}$$

This leads to the first expression of (3).

Appendix 2

Integration of the type of (13) is normally difficult, since the integrand is not single-valued because of the radicals $a = \pm\sqrt{k^2 - (\omega^2 - k\omega U)/c_p^2}$ and $b = \pm\sqrt{k^2 - (\omega^2 - k\omega U)/c_s^2}$ included. We avoid the difficulty by replacing the variable ω by a complex variable $\Omega = \omega_r + i\omega_i$ and introducing branch cuts to make the integrand single-valued. On the permissible sheet $\Re(a) > 0$ and $\Re(b) > 0$, where the factors e^{-az} and e^{-bz} do not diverge for large z.

The branch cuts should be given therefore by $\Re(a) = 0$ and $\Re(b) = 0$. For simplicity we examine the branch cuts for the case $U = 0$. For complex $\Omega = \omega_r + i\omega_i$ and $k = k_r + ik_i$,

$$\begin{aligned} a^2 &= (k_r^2 - k_i^2 + 2ik_rk_i) - (\omega_r^2 - \omega_i^2 + 2i\omega_r\omega_i)/c_p^2 \\ &= (k_r^2 - k_i^2) - (\omega_r^2 - \omega_i^2)/c_p^2 + 2i(k_rk_i - \omega_r\omega_i/c_p^2) \end{aligned} \tag{A2.1}$$

should be real and negative on the branch line (because a is pure-imaginary on $\Re(a) = 0$). Therefore,

$$\begin{aligned} k_rk_i &= \omega_r\omega_i/c_p^2 \\ k_r^2 - k_i^2 &< \frac{\omega_r^2 - \omega_i^2}{c_p^2}. \end{aligned} \tag{A2.2}$$

Likewise, from $\Re(b) = 0$,

$$\begin{aligned} k_rk_i &= \omega_r\omega_i/c_s^2 \\ k_r^2 - k_i^2 &< \frac{\omega_r^2 - \omega_i^2}{c_s^2}. \end{aligned} \tag{A2.3}$$

The branch points are located in the second and fourth quadrants as required from the condition that the contributions of the branch-line integrals corresponding to positive ω's should be obtained by contour-line integrals in the lower half plane

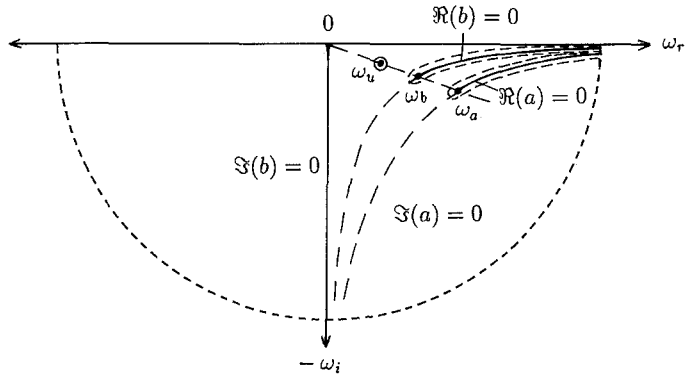

Figure A2.1
Illustration to explain the contour line for integration (13) in the text. A pole corresponding to the wave propagated with the landslide (ω_u) and two branch points (ω_a and ω_b) should be encircled by the contour in the negative-imaginary ω area. U is assumed to be zero.

(Fig. A2.1). From this condition k_i must be small negative for $k_r \geq 0$. Thus, by the two conditions, the branch points $\omega_a = c_p k$ and $\omega_b = c_s k$ are located in the fourth quadrant for positive k.

When the branch cuts in the fourth quadrant degenerate into a part of the real ω axis (Fig. A2.2), the net contributions from the branch line integrals are given only from the lower sides of branch cuts, since the contribution from the upper side of a contour toward the left is canceled out by that from the upper contour toward the right in contact with the former contour. The contributions from the branch-line integrals are proportional to $\exp(-az + ikx) = \exp(-a_r z - ia_i z + ikx)$. In the lower sides of the branch cuts $a_i < 0$, and the waves proportional to $\exp(-ia_i z + ikx)$ correspond to waves propagating away to the right and slightly upward from the basal layer.

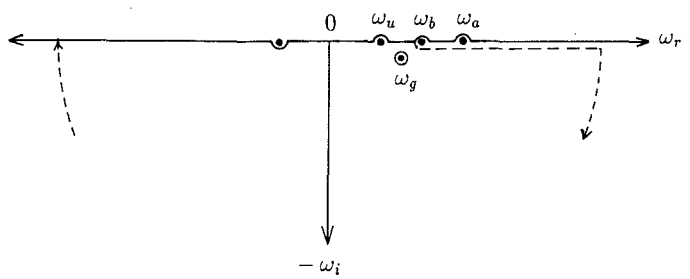

Figure A2.2
Contour line for integration (13) in the text when ω and k are taken as real. The pole corresponding to the guided wave along the basal zone (ω_g) is still complex and encircled by the contour. U is assumed to be zero.

The pole contribution by the guided wave is also obtained from that in the fourth quadrant, and the integral of the type,

$$\int_{-\infty}^{\infty} d\Omega, \tag{A2.4}$$

is conducted along the contour shown in Figures A2.1 or 2. The negative-imaginary ω part of the pole also implies body waves propagating away from the basal zone as explained for branch contributions.

Acknowledgement

I have undertaken this study stimulated by a hypothesis of *Basal Pressure Wave* by Mostafa A. Foda. During the work I benefited from discussions with Koji Yamada who was producing a computer simulation of the *Foda* model for his Master thesis study.

All the computations in this study were made with FACOM-M780 at the Data Processing Center, Kyoto University. This study was supported in part by a project for "the Scale and Characteristics of Volcanic Hazard," a grant in aid from the Ministry of Education and Culture represented by Professor S. Aramaki, Hokkaido University.

Criticisms of an anonymous reviewer were helpful in improving this paper.

REFERENCES

ASHIDA, K., and EGASHIRA, S. (1986), *Running-out Processes of the Debris Associated with the Ontake Landslide*, Natural Disaster Science *8*, 63–79.

BAGNOLD, R. A. (1954), *Experiments on a Gravity-free Dispersion of Large Solid Spheres in a Newtonian Fluid under Shear*, Proc. Roy. Soc. London *225A*, 49–63.

CLUFF, L. S. (1971), *Peru Earthquake of May 31, 1970; Engineering Geology Observations*, Bull. Seismol. Soc. Am. *61*, 511–533.

DAVIES, T. R. (1982), *Spreading of Rock Avalanche Debris by Mechanical Fluidization*, Rock Mechanics *15*, 9–24.

EASON, G. (1965), *The Stresses Produced in a Semi-infinite Solid by a Moving Surface Force*, Int. J. Eng. Sci. *2*, 581–609.

FODA, M. A. (1993), *Landslides Riding on Basal Pressure Waves*, to appear in Continuum Mechanics and Thermodynamics.

HABIB, P. (1975), *Production of Gaseous Pore Pressure during Rock Slides*, Rock Mechanics *7*, 193–197.

KENT, P. E. (1966), *The Transport Mechanism in Catastrophic Rock Falls*, J. Geology *74*, 79–83.

MELOSH, H. J. (1979), *Acoustic Fluidization: A New Geologic Process?*, J. Geophys. Res. *84* (B13), 7513–7520.

MELOSH, H. J. (1986), *The Physics of Very Large Landslides*, Acta Mechanica *64*, 89–99.

OKUDA, S., OKUNISHI, K., SUWA, H., YOKOYAMA, K., and YOSHIDA, R. (1985), *Restoration of Motion of Debris Avalanche at Mt. Ontake in 1984 and Some Discussions on its Moving State*, Disaster Prevention Res. Inst. Annuals, Kyoto Univ. *24A*, 491–504 (in Japanese).

PLAFKER, G., ERICKSEN, G. E., and CONCHA, J. F. (1971), *Geological Aspects of the May 31, 1970, Peru Earthquake*, Bull. Seismol. Soc. Am. *61*, 543–578.

SASSA, K. (1988), *Geotechnical Model for the Motion of Landslides*, Special lecture, Proc. 5th Intern. Symp. on Landslides, 37–55.

SCHEIDEGGER, A. E. (1973), *On the Prediction of the Reach and Velocity of Catastrophic Landslides*, Rock Mechanics *5*, 231–236.

SHREVE, R. L. (1968), *The Blackhawk Landslide*, Geol. Soc. Am. Spec. Paper *108*.

TAKARADA, S. (1991), *Flow and Depositional Mechanisms of Debris Avalanche—A Case Study of Iwasegawa Debris Avalanche Deposit, Tashirogawa Volcano, Northern Japan*, Bull. Volcanol. Soc. Japan *36*, 11–23 (in Japanese).